CHEMISTRY
A EUROPEAN JOURNAL

DOI: 10.1002/chem.200801607

Supramolecular Helical Fluid Columns from Self-Assembly of Homomeric Dipeptides

Channabasaveshwar V. Yelamaggad,*[a] Govindaswamy Shanker,[a] R. V. Ramana Rao,[b] Doddamane S. Shankar Rao,[a] Subbarao Krishna Prasad,[a] and Vommina V. Suresh Babu[b]

Abstract: Herein, we demonstrate that with the widespread theme of residue patterning and stereochemical restraints of self-complimenting proteinogenic amino acids, a new and rich class of homomeric dipeptides exhibiting two-dimensional fluid aggregates with hierarchical ordering can be obtained. In particular, a simple way of achieving a class of functional dipeptides, wherein the first and the second residues chosen are L-/D-alanines and L-/D-leucines, has been accomplished. The supramolecules synthesized can be regarded as intermediates between polycatenars and taper-shaped amphiphiles because they possess two lipophilic segments interlinked by a peptide unit (spacer). Two pairs of enantiomers and their respective diastereomers derived from these amino acids are evidenced to self-organize into a helical columnar phase through hydrogen bonding by means of FTIR, UV/Vis, and chiroptical circular dichroism (CD) spectral analyses as well as by optical, calorimetric, electrical switching, and X-ray studies. The CD and X-ray studies have revealed that the form chirality (handedness) and the magnitude of out-of-plane fluctuations of the lattice planes of the fluid supramolecular columnar structures are solely directed by the stereochemistry encoded in the spacer. Of special significance, the less frequently found oblique helical columnar phase formed by a pair of enantiomers derived from L-/D-alanines, unlike those derived from other amino acids, exhibit ferroelectric behavior; the measured spontaneous polarization is as high as 440 $nC\,cm^{-2}$. Besides, all these supramolecules form stable organogels in ethanol and the CD and SEM studies on a representative gel suggest the presence of helical structures.

Keywords: amino acids · gelation · hydrogen bonds · liquid crystals · peptides

Introduction

Molecular self-assembly, a prevailing means of generating novel networks that combine several properties and respond to external stimuli, has great significance in biological and material sciences.[1] Columnar (Col) liquid-crystal (LC) phases[2] built up by the self-organization of columns of indefinite length into two-dimensional lattices with different symmetries are examples of such novel structures. Generally, fluid columns result from the noncovalent interactions of a variety of molecular architectures, such as discotics,[2,3] bent-core molecules,[4] polycatenars,[5] and dendrimers,[6] as shown in Figure 1. However, to achieve even greater structural order and complexity in these fluid 2D motifs with selectivity, directionality, reversibility as well as the possibility of controlling the strength of the interactions through self-assembly and intermolecular hydrogen bonding, supramolecules such as amphiphiles,[7] bolaamphphiles,[8] amides,[9,10,11a–e,12,13] hydrazides,[11f] and peptides,[14–16] seem to be the most promising and advanced approach.

Of these supramolecules, biocompatible polypeptides[14] and low molar mass peptides[15,16] have been attracting a great deal of attention owing to their ability to form thermotropic or lyotropic Col phases with a variety of supramolecular structures. For example, poly(γ-*n*-alkyl-L-glutamate), which has an intrinsic rigid α-helical chain resulting from

[a] Dr. C. V. Yelamaggad, G. Shanker, Dr. D. S. S. Rao, Dr. S. K. Prasad
Centre for Liquid Crystal Research
Jalahalli, Bangalore 560013 (India)
Fax: (+91) 80-2838-2044
E-mail: Yelamaggad@gmail.com

[b] Dr. R. V. R. Rao, Prof. V. V. S. Babu
Department of Studies in Chemistry
Central College Campus
Bangalore University, Bangalore 560001 (India)

Supporting information for this article is available on the WWW under http://dx.doi.org/10.1002/chem.200801607.

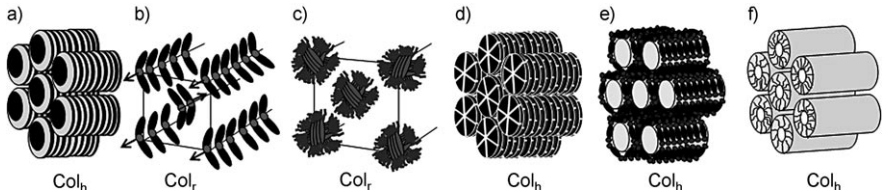

Figure 1. Models of fluid columns formed by different molecular architectures, such as a) discogens, b) bent-core systems (the bow/polar axes, indicated by an arrow, are along the column axis), c) polycatenars, d) dendrimers or amides, e) bolaamphiphiles, and f) polypeptides. Col_h = hexagonal columnar phase, Col_r = rectangular columnar phase.

the intramolecular hydrogen-bonding network of constituent amino acid (monomers) residues, aggregates into a 2D hexagonal lattice.[12] Several low molar mass, but polymerizable, Brønsted acidic (amides) amphiphiles preferentially form the inverted hexagonal (H_{II}) lyotropic LC phase.[13] Semifluorinated twin dendritic benzamides are shown to self-organize into bilayered pyramidal supramolecular columns.[14] Recently, a large number of dendritic (depsi) dipeptides have been realized and are shown to self-assemble into porous and supramolecular Col structures.[15] Notably, Col LCs formed by depsipeptides[16] derived from folic acid and/or glutamic acid residues are regarded as the biocompatible fluids for use in membranes and sensors. Herein, we demonstrate for the first time that, with the widespread theme of residue patterning and stereochemical restraints of self-complementing proteinogenic amino acids,[17] a new and rich class of homomeric oligopetides exhibiting two-dimensional fluid aggregates with hierarchical ordering can be obtained. Thereby, anisotropic functional materials can be accomplished in which many important features, such as chirality, ferroelectric behavior, gelating capabilities, and biocompatibility, can be incorporated that are attractive from the view points of both life science and technologically important materials. For this purpose, a number of aspects were considered to give such systems a synthetic and structural versatility, whilst maximizing the probability of mesophase stabilization. In particular, supramolecules consisting of two lipophilic (*n*-trialkoxybenzene) segments interlinked through a peptide unit (spacer), and thus, representing the features of both hexacatenars and taper-shaped amphiphiles were designed. Such a design should also help in understanding the structure–property relationship, which can be extrapolated to know the behavior of macromolecules. Thus, as a first step in this direction, a simple way of achieving a new class of materials was conceived for the synthesis of dipeptides in which the first and the second residues may be any one of the amino acids available, yielding a large number of distinct dipeptides. In this study, L-/D-alanines and L-/D-leucines are chosen to form dipeptide sequences to achieve the targets. The analogous but representative dipeptides substituted with mono- and dialkoxy tails on each of the benzene cores were also prepared to support the point that the space-filling concept is essential to realize fluid columnar organization.

Results and Discussion

Synthesis: The proposed enantiopure oligomers were synthesized in six simple and high yielding steps using the key intermediates shown in Scheme 1. The coupling of appropriate N^{α}-Fmoc amino acids (Fmoc = 9-fluorenylmethoxycarbonyl; **27a**,**b** and **28a**,**b**) with various *n*-alkoxyanilines (**21**–**23**) in the presence of *N*-methylmorpholine (NMM) and isobutoxycarbonyl chloride (IBC-Cl) gave Fmoc amino acid amides **17**–**20**; these amides, upon treatment with a 1:1 mixture of diethylamine/dichloromethane, gave amines **13**–**16**. The amines obtained were coupled with N^{α}-Fmoc amino acids **27a**,**b** and **28a**,**b** by using NMM and IBC-Cl to obtain protected dipeptides that were deprotected under the same reaction conditions mentioned previously to obtain key amines **5**–**8**. Finally, target molecules **1**–**4** were formed in excellent yields when *n*-alkoxybenzoic acids (**24**–**26**) were coupled with amines **5**–**8** in the presence of 2-(1*H*-benzotriazol-1-yl)-1,1,3,3-tetramethyluronium hexafluorophosphate (HBTU). It is appropriate to mention here that key amines **5**–**8** and **13**–**16**, unlike other intermediates (**9**–**12** and **17**–**20**), were isolated in quantitative yields and used directly in the next step. The molecular structure of the peptides were assessed by UV, FTIR, ^{1}H, and ^{13}C NMR spectroscopies; mass spectrometry; and elemental analyses (see the Supporting Information). Notably, the ^{1}H–^{1}H COSY NMR spectroscopy profile illustrated coupling between the NH and methine proton of the peptide chain (see the Supporting Information for details), which supported the structural assignment.

Infrared, UV/Vis, and circular dichroism (CD) spectroscopic studies: The FTIR spectra of the dipeptides indicated the existence of strong intermolecular hydrogen bonding in both the solid (see the N−H and C=O stretching vibrations given in the Experimental Section and also the Supporting Information for more information) and LC states. For example, a thin film of **3a** sandwiched between the KBr plates was cooled from the isotropic phase to room temperature, and the FTIR spectrum was recorded at regular temperature intervals. As expected, as the temperature decreased two broad bands at around 3281 and 1633 cm^{-1} due to N−H and C=O stretching vibrations, respectively, became stronger (increased in intensity) and were pronounced near room temperature (see the Supporting Information). These results clearly indicate the hydrogen-bonding interaction between the NH and CO groups, which become progressively stronger on going from the isotropic phase to the mesophase, and further to the glassy state.[11b,17c] In addition, disordering of the *n*-alkoxy tails present on either side of the dipeptide was indicated by the observation of asymmetric and symmetric C−H stretching bands at 2937 and 2858 cm^{-1}, respectively.[11f]

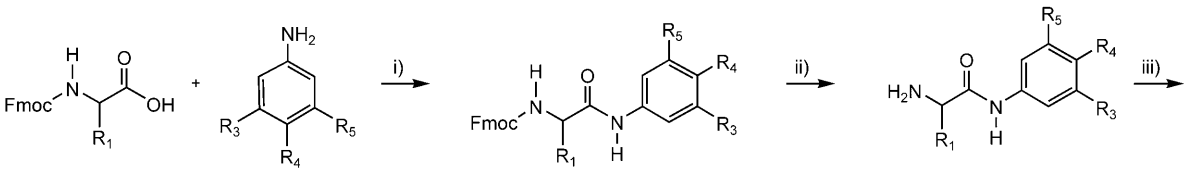

27a: R_1= (*S*)-Me
27b: R_1= (*R*)-Me
28a: R_1= (*S*)-*i*Bu
28b: R_1= (*R*)-*i*Bu

21: R_3= R_5= H; R_4= $OC_{10}H_{21}$
22: R_3= H; R_4=R_5 = $OC_{10}H_{21}$
23: R_3=R_4= R_5 = $OC_{10}H_{21}$

17: R_1= (*S*)-*i*Bu; R_3= R_5= H; R_4 = $OC_{10}H_{21}$
18: R_1= (*S*)-*i*Bu; R_3= H; R_4=R_5 = $OC_{10}H_{21}$
19a: R_1= (*S*)-Me; R_3=R_4=R_5 = $OC_{10}H_{21}$
19b: R_1= (*R*)-Me; R_3=R_4=R_5 = $OC_{10}H_{21}$
20a: R_1= (*S*)-*i*Bu;R_3=R_4=R_5 = $OC_{10}H_{21}$
20b: R_1= (*R*)-*i*Bu;R_3=R_4=R_5 = $OC_{10}H_{21}$

13: R_1= (*S*)-*i*Bu; R_3= R_5= H; R_4 = $OC_{10}H_{21}$
14: R_1= (*S*)-*i*Bu; R_3= H; R_4=R_5 = $OC_{10}H_{21}$
15a: R_1= (*S*)-Me; R_3=R_4=R_5 = $OC_{10}H_{21}$
15b: R_1= (*R*)-Me; R_3=R_4=R_5 = $OC_{10}H_{21}$
16a: R_1= (*S*)-*i*Bu;R_3=R_4=R_5 = $OC_{10}H_{21}$
16b: R_1= (*R*)-*i*Bu;R_3=R_4=R_5 = $OC_{10}H_{21}$

9: R_2 = R_1 = (*S*)-*i*Bu; R_3 = R_5 = H; R_4 = $OC_{10}H_{21}$
10: R_2 = R_1 = (*S*)-*i*Bu; R_3 = H; R_4 = R_5 = $OC_{10}H_{21}$
11a: R_2 = R_1 = (*S*)-Me; R_3 = R_4 = R_5 = $OC_{10}H_{21}$
11b: R_2 = R_1 = (*R*)-Me; R_3 = R_4 = R_5 = $OC_{10}H_{21}$
11c: R_2 = (*R*)-Me; R_1 = (*S*)-Me; R_3 = R_4 = R_5 = $OC_{10}H_{21}$
12a: R_2 = R_1 = (*S*)-*i*Bu; R_3 = R_4 = R_5 = $OC_{10}H_{21}$
12b: R_2 = R_1 = (*R*)-*i*Bu; R_3 = R_4 = R_5 = $OC_{10}H_{21}$
12c: R_2 = (*R*)-*i*Bu; R_1 = (*S*)-*i*Bu; R_3 = R_4 = R_5 = $OC_{10}H_{21}$

5: R_2 = R_1 = (*S*)-*i*Bu; R_3 = R_5 = H; R_4 = $OC_{10}H_{21}$
6: R_2 = R_1 = (*S*)-*i*Bu; R_3 = H; R_4 = R_5 = $OC_{10}H_{21}$
7a: R_2 = R_1 = (*S*)-Me; R_3 = R_4 = R_5 = $OC_{10}H_{21}$
7b: R_2 = R_1 = (*R*)-Me; R_3 = R_4 = R_5 = $OC_{10}H_{21}$
7c: R_2 = (*R*)-Me; R_1 = (*S*)-Me; R_3 = R_4 = R_5 = $OC_{10}H_{21}$
8a: R_2 = R_1 = (*S*)-*i*Bu; R_3 = R_4 = R_5 = $OC_{10}H_{21}$
8b: R_2 = R_1 = (*R*)-*i*Bu; R_3 = R_4 = R_5 = $OC_{10}H_{21}$
8c: R_2 = (*R*)-*i*Bu; R_1 = (*S*)-*i*Bu; R_3 = R_4 = R_5 = $OC_{10}H_{21}$

24: R_3= R_5= H;R_4= $OC_{10}H_{21}$
25: R_3= H; R_4=R_5 = $OC_{10}H_{21}$
26: R_3=R_4= R_5 = $OC_{10}H_{21}$

1: R_2 = R_1 = (*S*)-*i*Bu; R_3 = R_5 = H; R_4 = $OC_{10}H_{21}$
2: R_2 = R_1 = (*S*)-*i*Bu; R_3 = H; R_4 = R_5 = $OC_{10}H_{21}$
3a: R_2 = R_1 = (*S*)-Me; R_3 = R_4 = R_5 = $OC_{10}H_{21}$
3b: R_2 = R_1 = (*R*)-Me; R_3 = R_4 = R_5 = $OC_{10}H_{21}$
3c: R_2 = (*R*)-Me; R_1 = (*S*)-Me; R_3 = R_4 = R_5 = $OC_{10}H_{21}$
4a: R_2 = R_1 = (*S*)-*i*Bu; R_3 = R_4 = R_5 = $OC_{10}H_{21}$
4b: R_2 = R_1 = (*R*)-*i*Bu; R_3 = R_4 = R_5 = $OC_{10}H_{21}$
4c: R_2 = (*R*)-*i*Bu; R_1 = (*S*)-*i*Bu; R_3 = R_4 = R_5 = $OC_{10}H_{21}$

Scheme 1. i) NMM, isobutoxycarbonyl chloride, THF, 0°C→RT, 10 h, 70–74%; ii) diethylamine/dichloromethane (1:1), RT, 2 h, quantitative; iii) **27a**, **27b**, **28a**, or **28b**, NMM, isobutoxycarbonyl chloride, THF, 0°C→RT, 12 h, 68–70%; iv) **5**, **6**, **7a–c**, or **8a–c**, HBTU, THF, *N*-ethyldiisopropylamine, 70–72%.

Owing to the presence of multiple chromophores and hydrogen bonds, these dipeptides are expected to exhibit interesting photophysical properties. Thus, UV/Vis absorption and CD spectroscopic studies were carried out. The solution UV/Vis spectra (in CH_2Cl_2) of all of the compounds showed an absorption maxima centered at around 260 nm (see the Supporting Information); as representative examples, the solution UV/Vis spectra for **4a** and **4b** are shown in Figure 2a. CD measurements carried out at 23°C for dilute solutions of all the dipeptides (7.3×10^{-5} M in CH_2Cl_2; cell length = 1 mm) showed a significant Cotton effect, establishing the supramolecular chirality of the aggregates, wherein molecules self-assemble into helical arrays through the hydrogen bonding of successive peptide chains. For example, as shown in Figure 2b, enantiomeric peptides **4a** and **4b** exhibit, as anticipated, mirror-image Cotton effects with the absorption bands at λ = 242 (molar ellipticity = −12.1), 273 (molar ellipticity = +11.4), 239 (molar ellipticity = +10.6), and 275 nm (molar ellipticity = −13.4). The zero crossing in both cases is close to the absorption maximum of the chromophores ($\lambda \approx 260$ nm; Figure 2a), which indicates exciton coupling due to dipeptides aggregated through hydrogen bonds to generate a helical (chiral) superstructure. To investigate whether molecular chirality coupled with hydrogen bonding has facilitated the self-assembly of dipeptides into fluid helical columns, qualitative CD measurements were carried out for

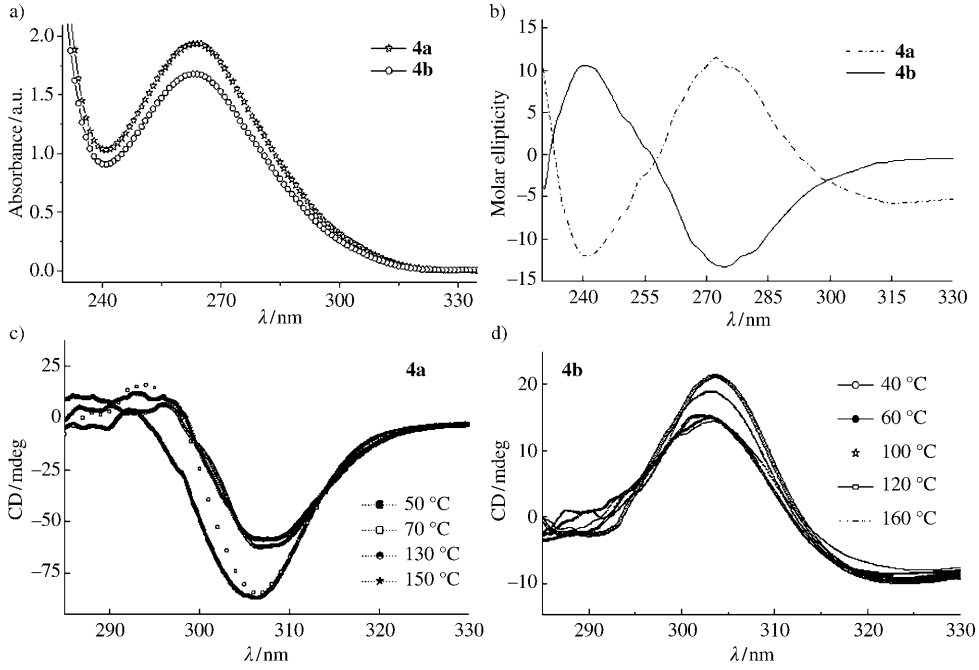

Figure 2. UV/Vis (a) and CD (b) spectra obtained for the dilute solutions of dipeptides **4a** and **4b**. The CD spectra obtained in the mesophases as a function of temperature for dipeptide **4a** (c) and **4b** (d) are also shown. Note that the enantiomeric pairs exhibited mirror image CD curves in both solution and mesophase states.

the enantiomeric pairs **3a**/**3b** and **4a**/**4b**. These compounds, held between two quartz plates, were heated to their isotropic phase and cooled slowly, during which time the CD spectra were recorded at selected temperatures; notably, all the fluid phases displayed the Cotton effect, which signified large chiral correlations in the molecular packing.[11] In particular, each of the enantiomeric pairs exhibited mirror-image CD curves, as illustrated in Figure 2c and d for compounds **4a** and **4b** as representative examples (see the Supporting Information for the CD plots of **3a** and **3b**). It can be seen that the intensity of the CD signals increases with the decrease in temperature. Thus, from the results above, it is evident that these dipeptides form helical aggregates in solution and/or mesophase states governed by the nature of the substituent and its orientation (stereochemistry) in the peptide linkage.

Mesomorphic behavior: The thermal behavior of dipeptides **1**–**4**, ascertained with the aid of optical polarizing microscopy (OPM), differential scanning calorimetry (DSC), and X-ray diffraction (XRD) studies, is summarized in Table 1. Compounds **1** and **2**, comprising of dialkoxy and tetraalkoxy tails, respectively, fail to exhibit LC behavior. In contrast, dipeptides **3a**–**c** and **4a**–**c**, with hexaalkoxy tails, display Col LC behavior, which supports our design view that space filling is essential.

These compounds with three distinct, incompatible regions (paraffinic tails, aromatic cores, and a peptide spacer) can be termed amphiphilic hexacatenars. Most importantly, the nature (stereochemical restrains) of the central peptide segment in the molecules dictates their packing, which in turn reflects on the magnitude of out-of-plane fluctuation of the lattice plane. Enantiomers **3a** and **3b** exhibit an identical and enantiotropic mesophase. When placed between clean glass plates and cooled from the isotropic phase (**3a**: 175.1 °C, $\Delta H = 5.9\ J\,g^{-1}$; **3b**: 176.6 °C, $\Delta H = 6.5\ J\,g^{-1}$) these samples display dendritic growth, as shown in Figure 3a and b, that quickly fills the field of view and remains unaltered up to room temperature (RT). The dendritic textural pattern suggests that the mesophase is a Col phase. The Col phase, once formed upon melting, does not crystallize and instead it freezes into a glassy state and exists for a wide thermal range, as established by both optical and calorimetric studies; the textural pattern obtained remains as such for any period of time and no exothermic (from just below the Iso–Col phase transition to −60 °C) or endothermic (from −60 °C to near the Col–Iso phase transition) peaks were seen in the first cooling or second heating DSC profiles, respectively. Figure 4 depicts the DSC profiles obtained for compound **3a**, in which the above-mentioned features are seen. The 2D glassy state featuring a helical order, as evidenced by CD measurements, is of special importance because in such a state the charges

Table 1. Transition temperatures [°C] and enthalpies [Jg^{-1}] of peptides.[a]

Dipeptides	Phase sequence	
	Heating	Cooling
1	Cr_1 136.6 (33.6) Cr_2 142.1 (185.7) > 320 I	–
2	Cr_1 79.2 (3.6) Cr_2 130.9 (32.9) I[b]	–
3a	Cr 51.1 (35.8) Col_{ob} 181.1 (6.7) I	I 175.1 (5.9) Col_{ob}[c]
3b	Cr 52.5 (29.9) Col_{ob} 181.1 (7) I	I 176.6 (6.5) Col_{ob}[c]
3c	Cr 76 (6.6) Col_r 102.3 (6.3) I	I 89.4 (6.3) Col_r[c]
4a	Cr_1 49.7 (17.4) Cr_2 220.1 (1.1) Col 228.1 (7) I	I 221 (6.4) Col 191 (2) Cr
4b	Cr 218.5 (2.6) Col 228.1 (14.8) I	I 224.6 (10) Col 197.8 (2.6) Cr
4c	Cr 90.9 (12.2) I	I 80 (6) M 78.1 (5) Col_r 24.1 (1.4) Cr

[a] Peak temperatures in the DSC thermograms obtained during the first heating and cooling cycles at 5 °C min^{-1}. Col_{ob} = oblique columnar phase, Col_r = rectangular columnar phase, M = unidentified mesophase, I = isotropic liquid phase, Cr_1 and Cr_2 = crystal. [b] Upon cooling the isotropic liquid, the sample freezes into glassy state. [c] The phase exists (supercools) up to the limit of the DSC (−60 °C) instrument.

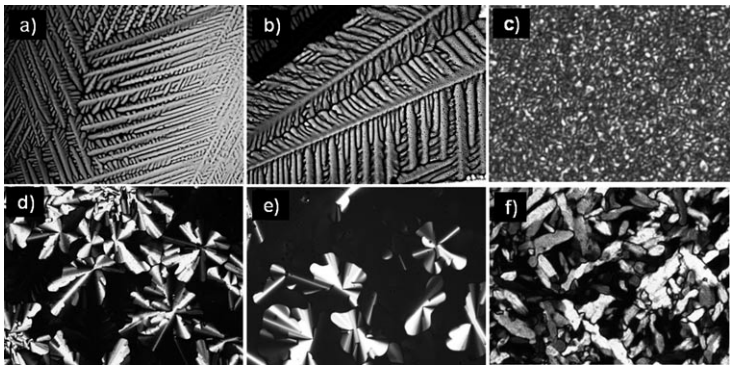

Figure 3. Microphotographs of the optical textures obtained for the Col_{ob} phase of **3a** at 170 °C (a) and **3b** at 177 °C (b); the Col_r phase of **3c** at 88 °C (c), **4a** at 205 °C (d), **4b** at 200 °C (e), and **4c** at 60 °C (f).

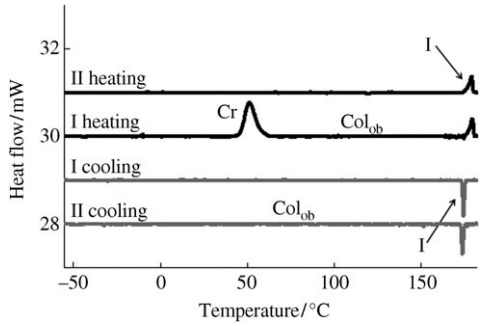

Figure 4. DSC thermograms of amphiphilic dipeptide **3a** obtained at a rate of 5 °C min^{-1}.

generated flow smoothly at the expense of the motion of the ionic impurities.[6]

The powder XRD patterns obtained in the mesophase of both compounds at different temperatures, including RT, were found to be almost identical (see the Supporting Information). In all of the profiles, a typical diffuse peak occurring at high angles ($2\theta \approx 20°$, spacing $c = 4.51$ Å) indicates the fluid nature of the phase (Table 2). In the low-angle region, a number of sharp and intense peaks were seen, a feature that indicates long-range order of the 2D lattice. As a representative example the 2D diffraction pattern (Figure 5a) and the derived one-dimensional intensity versus 2θ profile (Figure 5b) of an unoriented (powder) sample of the Col phase formed by **3a** are shown. First, we note that the ratio of the two lowest angle peaks is 1.1, a value that is inconsistent with a hexagonal lattice for which the ratio should be 1.73 ($\sqrt{3}$). As can be seen from Table 2, such a deviation is true for all the dipeptides derived from alanine studied herein and rules out the hexagonal lattice. Next, we performed indexation of the reflections using a least-squares method. Table 2 lists the d-spacing values obtained experimentally and calculated from indexed lattices and it is seen that deviations between the two are generally small. An appropriate fitting of the data for compounds **3a** and **3b** point to an oblique lattice. Forcing the fit to a rectangular lattice results in a considerable increase in the cumulative error.

Table 2. Results of indexation of XRD profiles at a given temperature of phases displayed by the dipeptides **3a–c** and **4a–c**. (The negative sign in front of the miller index digit indicates an overline).

Dipeptides	T [°C]	Phase	d_{exp} [Å]	d_{calcd} [Å]	Miller index	Lattice parameters [Å]
3a	100	Col_{ob}	25.69	25.65	20	$a = 51.6$
			23.66	23.37	21	$b = 45.2$
			21.27	21.31	−21	$\gamma = 83.9$
			19.88	19.80	−12	
			16.21	16.06	−22	
			14.41	14.36	32	
			13.38	13.57	23	
			10.69	10.71	−33	
			4.51			
3b	100	Col_o	25.75	25.65	20	$a = 51.7$
			23.66	23.50	21	$b = 45.6$
			20.87	21.15	−21	$\gamma = 82$
			19.74	19.59	−12	
			16.09	15.90	−22	
			14.45	14.44	32	
			13.26	13.59	23	
			10.65	10.63	−14	
			9.53	9.74	−51	
			4.57			
3c	80	Col_r	31.82	31.80	11	$a = 52.5$
			26.22	26.23	20	$b = 40$
			17.43	17.49	30	
			16.32	16.02	31	
			4.45			
4a	210	Col	22.77		11	
			8.50		20	
			4.66		03	
			4.63		32	
4b	210	Col	22.72		11	
			8.48		20	
			4.67		03	
			4.62		32	
4c	70	Col	19.23	19.07	11	$a = 32.2$
			16.24	16.11	20	$b = 23.7$
			13.50	13.31	21	
			11.90	11.83	02	
			10.35	11.1	12	
			9.96	9.78	31	
			8.92	9.53	22	
			8.05	8.05	40	
			7.68	7.66	13	
			7.00	7.08	23	
			6.67	6.66	42	
			4.53			
			3.86			

Therefore, we assign the lattice (for both **3a** and **3b**) to be an oblique one. The unit cell volume increases by approximately 4% when the temperature is increased from 100 to 160 °C, and is accompanied by an increase in h as well as the cell area. Assuming the density to be 1 g cm^{-3} the lattice parameters suggest four molecules per unit cell. A possible molecular configuration involving these features and with polar properties is shown in Figure 6c.

Interestingly, this phase does not exhibit an X-ray peak that is typical in systems possessing a finite, albeit short range, interaction between the rigid cores of the neighboring molecules of the same column. Therefore, the structure has an extremely well-defined 2D lattice, but hardly any posi-

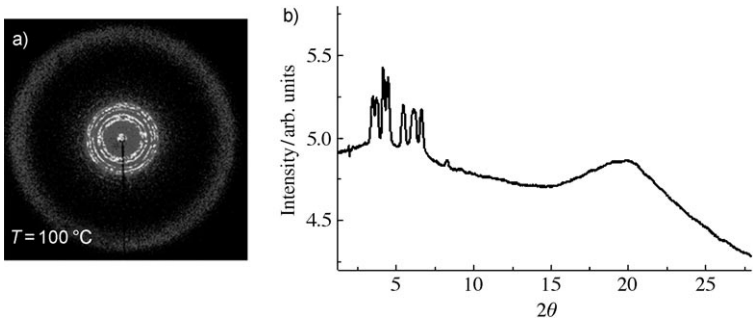

Figure 5. Two-dimensional XRD pattern (a) and the derived 1D-intensity versus 2θ profile (b) for the Col_{ob} phase of dipeptide **3a**.

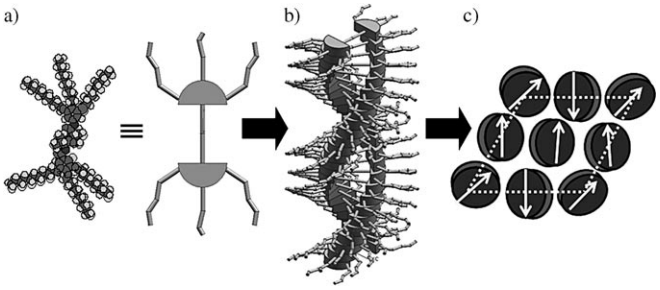

Figure 6. a) Molecular (with a schematic) model of **3a** in its all-*trans* conformation (front view), b) schematic representation of a supramolecular column (lateral view) in which peptide molecules organize in a helical fashion, and c) a possible lattice (the arrows indicate the direction of the dipole moment).

tional order perpendicular to the lattice plane. The reason for the absence of positional ordering could be that unlike in conventional discotics the central region in the present molecule is not a rigid core.[18] The fact that a Cotton effect could be observed in the Col phase establishes that the structural organization is due to intermolecular hydrogen bonding between the hexacatenar-like mesogens (Figure 6a) within the same column causing a helical array as shown in Figure 6b (in this model, for convenience, the two terminal phenyl rings are sketched to be planar; needless to say, these two rings are otherwise free to rotate). Further, such indefinitely long columns in turn self-organize to form a Col phase with the cell parameters discussed above (a possible lattice is shown in Figure 6c, which is also one of the possibilities suggested for another ferroelectric Col phase[22c]). It may be recalled that such Col structures with a helical arrangement are seen in chiral molecules self-assembled in a solvent medium.[19a] It may be emphasized that in the present case the self-assembly occurs in a solvent-free medium.[19b]

Dipeptide **3c** resulting from coupling D- and L-alanine residues displayed a mesophase with different textural and XRD patterns than those obtained for its diastereomers **3a** and **3b**. An enantiotropic mesophase, which on cooling from the Iso phase shows a noncharacteristic texture (Figure 3c) for any surface-anchoring condition, exists over a wide thermal range and does not crystallize. In the XRD profile, the number of sharp reflections (Table 2 and the Supporting Information) in the low-angle region is reduced to four. While the hexagonal lattice is ruled out on the basis of the ratio of the spacings of the first two reflections, fitting to an oblique lattice ($a=65.4$ Å, $b=34.2$ Å and $\gamma=76.6°$) and rectangular columnar lattice with the unit cell parameters $a=52.5$ Å and $b=40$ Å were considered. However, fitting to the oblique lattice yielded an increased cumulative error. Therefore, we believe the lattice to be rectangular. Further, since the h and k values are such that $h+k$ is odd as well as even, a centered lattice is ruled out. Therefore, we suggest that the space group is $P2_1$. Of course, a diffuse reflection is seen at wide angles centered at a spacing of around 4.4 Å, indicating liquidlike ordering.

Homomeric dipeptides **4a** and **4b**, constructed from two L-leucine and two D-leucine residues, respectively, exhibit an identical but enantiotropic Col phase, as revealed by optical, calorimetric, and XRD studies. The optical texture was a combination of pseudofocal conic fan-shaped defects, and homeotropic digitated stars (Figure 3d and e), which is typical of the Col phase; we faced a problem indexing the lattices, since only two sharp reflections were seen with spacings of 22.77 and 8.5 Å for **4a**, and 22.72 and 8.48 Å for **4b**. Therefore, no assignment is made to the lattice structure for the Col of dipeptides **4a** and **4b**. Further, an unusual broad peak occurring at around $2\theta=6°$ was seen (Figure 7). Note that such a feature has also been reported for hexaazatrinaphthylene[20] and polycatenar[21] mesogens, and attributed to the height of a Col segment.

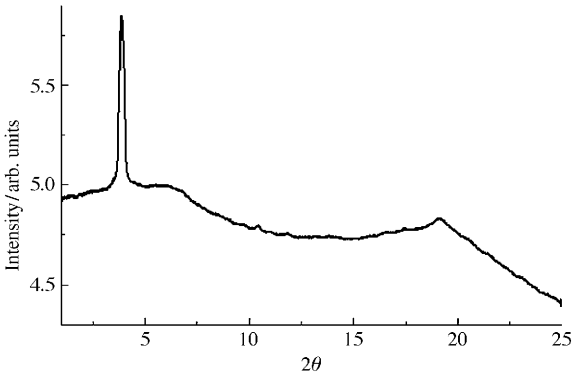

Figure 7. One-dimensional intensity versus 2θ profile derived from the two-dimensional XRD pattern obtained at 210°C for the Col phase of compound **4a**.

Dipeptide **4c**, possessing D- and L-leucine residues, stabilizes two monotropic mesophases unlike its diastereomers **4a** and **4b**. When the thin film of an isotropic liquid of com-

pound **4c** held between clean glass slides was cooled slowly, a transition to the mesophase (hereafter referred to as M) occurs with uncharacteristic grainy texture of low birefringence; this was true even when slides treated for planar or homeotropic alignments were used. Because of the short thermal range of the phase, its structural elucidation by X-ray investigations was not successful. However, the identity of the Col phase occurring below the M phase was confirmed by OPM and XRD studies. It showed an optical texture pattern consisting of both pseudofocal conic fan-shaped defects and a homeotropic region typical of the Col phase. In the low-angle region, a set of sharp reflections was obtained and here again we rule out the hexagonal lattice owing to the small ratio of the first two low-angle reflections. This is supported by the presence of the 210 reflection, which is inconsistent with the hexagonal symmetry. A hexagonal cell can be treated as equivalent to a C-centered orthorhombic cell with the lattice constants satisfying the condition $a=b\sqrt{3}$. But for a C-centered lattice the reflections with an odd value for $h+k$ must be systematically absent, a feature not corroborated by the data in Table 2 (also note that the (21) reflection is quite intense). This feature is, however, possible if there is an alternation in the tilt direction so as to give a herringbone-type of arrangement, with the space group $P2_1a$ and two molecules per unit cell. Unlike the compounds derived from alanine, the leucine derivatives exhibited, in the wide-angle region, two broad diffuse peaks well separated in the case of **4c**. While the slightly lower angle one with a spacing of approximately 4.5 Å is due to a correlation between aliphatic chains, the higher angle one indicates the correlation of the molecular cores within the same column. It is interesting to see that diastereomer **4c** has the closest packed (3.8 Å) cores.

It is quite prominent that enantiomers **3a**,**b** and **4a**,**b** and their respective diastereomers **3c** and **4c** profoundly differ not only in their phase-transition temperatures, but also in the extent of lattice formation of the columnar phase. Most strikingly, the Col–Iso transition temperatures are quite high ($>180\,^{\circ}C$) for enantiomeric pairs **3a**,**b** and **4a**,**b**, when compared with their respective diastereomers **3c** and **4c** (Col–Iso $<100\,^{\circ}C$). The important difference between these supramolecules is the stereochemical feature of the peptide chain (spacer) resulting from the size and orientation (chirality) of the substituent of the amino acid components present, which affects the extent of hydrogen-bond formation in the resulting supramolecular structure. The presence of two substituents on either side of the peptide chain enforces thorough and strong intermolecular hydrogen bonding for compounds **3a**,**b** or **4a**,**b** leading to interactions between the supramolecules of the column that reflects on the overall columnar structure. Thus, it is noteworthy that these novel homomeric dipeptides form oblique or rectangular columnar structures, indicating that these hexacatenar architectures possessing three sufficiently incompatible subunits provide a powerful design principle for creating new and diverse fluid superstructures from supermolecules. In essence, the formation of supramolecular columns with form chirality can be ascribed to occurrence of multiple hydrogen bonds between N–H and C=O groups and subtle microphase segregation among the heterogeneous molecular fragments.

Electro-optical switching: From the symmetry arguments, all the tilted columns formed from chiral disklike molecules are expected to show ferroelectric behavior as the columns are spontaneously polarized perpendicular to the plane containing the column axis and the disk normal. Surprisingly, the majority of tilted columns consisting of chiral disklike molecules are apolar (nonswitchable); except for a few examples,[22–25] all known discotics exhibiting a polar columnar phase possess *O*-alkyl-lactic acid chains that create strong tilt-induced dipoles.[22e,f] Given the fact that the dipeptides of the present investigation exhibit a columnar phase composed of chiral supramolecules, they were tested for ferroelectric behavior. For this purpose, samples contained between ITO-coated glass plates were cooled slowly from the isotropic phase. Then the electro-optic switching features were observed under the OPM. To ascertain the ferroelectric nature of the mesophase, as well as to determine the spontaneous polarization (P_s), a triangular wave field was used. Only the Col_{ob} phase of **3a**–**3b** could be switched, which we describe as follows: On application of a triangular wave field (64 V, 10 Hz; thickness of the cell 8.5 μm) the Col phase of **3a**–**3b** showed a single peak per half cycle of the field (Figure 8a), indicating the ferroelectric nature; the peak vanishes in the isotropic phase ruling out any ionic origin. When the sample cell was oriented such that one of the states has minimum intensity between crossed polarizers, there is a change in the birefringence when the polarity reversal of the field switches the other state (see Figure 8b and c). To further support the argument that the switching is due to the ferroelectric character, we monitored the light transmission from the sample kept between crossed polarizers. Upon application of a square wave field, a sharp variation in the sample transmission is seen as shown in Figure 8d.

A feature observed is that the switching is actually bistable; the field-achieved state would remain intact after the removal of the field. As the CD measurements show that the columns are helical, the above observation suggests that the helix would have unwound, perhaps due to a phenomenon similar to surface stabilized for the smectic ferroelectrics. The combined area under the current response peak is a direct measure of the P_s and was found to be 440 $nC\,cm^{-2}$; this is analogous to the chiral smectic (SmC*) phase exhibited by chiral rodlike molecules or their mixtures.

Gelation study: Gels, formed by the noncovalent interaction between the gelator (organic or inorganic) and solvent molecules, are of great significance in both life science and materials chemistry.[26–29] Owing to their promising features in various applications, a considerable amount of work focusing on the design and preparation of a variety of functional gels has been witnessed. For example, the gels derived from LC phases (nematic or smectic)[27] or mesogens (calamitics

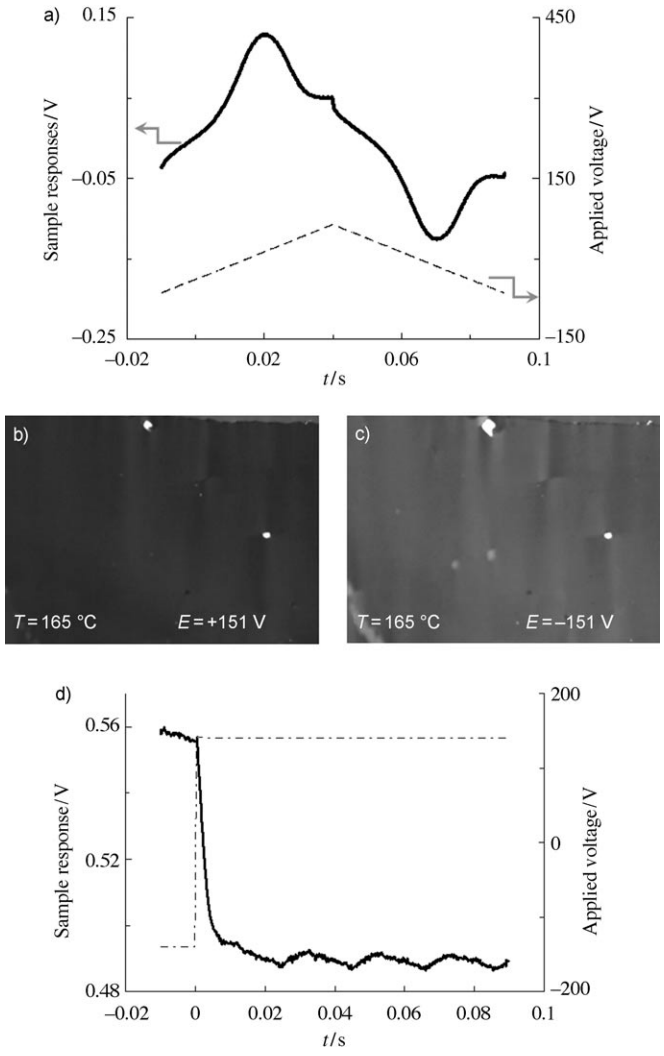

Figure 8. a) Ferroelectric switching current response trace obtained for the Col_{ob} phase of **3a** (triangular wave field, 64 V, 10 Hz). b, c) Microphotographs of the two bistable states. d) Optical response showing a sharp change in the intensity associated with a change in the sign of the applied square wave field (143 V, 1 Hz, ——: sample response, –•–•: applied voltage).

tides was carried out; it was found that they readily form stable gels in ethanol. The aprotic solvents do not seem to favor the formation of gels. Herein, we describe the gelation property of dipeptide **3b** as a representative example. A mixture of dipeptide **3b** (50 mg) and absolute ethanol (1 mL) was warmed in a capped vial until the solid dissolved. The undisturbed clear solution obtained was allowed to cool to room temperature during which time the gel was formed. The formation of the gel was ascertained by the test tube inversion method, as illustrated in Figure 9a. The sol-to-gel phase transition was found to be thermally reversible. The FTIR spectrum of the gel showed the stretching vibration of N–H and C=O at 3369 and 1624 cm^{-1}, respectively; additionally, the absorption band arising from the asymmetric ν_{as}(C–H) and symmetric ν_{s}(C–H) stretching vibrations of the alkyl chains at 2974 and 2849 cm^{-1}, respectively, were also observed. These results clearly indicate a strong interaction of the dipeptide (gelator) and the protic solvent through hydrogen bonds. The gel, sandwiched between two quartz plates, was investigated by CD spectroscopy at ambient temperature to learn about whether the soft macroscopic structure features the form chirality: the helical organization. Indeed, the Cotton effect was observed; the CD spectra consisted of two broad negative bands at 301 (−4.9 mdeg) and 225 (−16 mdeg) suggesting the intermolecular interactions between two or more electronic transition dipoles arranged in a helical order (see the Supporting Information for details).

The scanning electron microscopic (SEM) images (Figure 9b, c) were obtained to learn about the morphology of the formed gel qualitatively. The images revealed the occurrence of a 3D network comprising fibers featuring a right-handed twist. Therefore, it may be reasonable to presume that the formation of a 3D network (gel) of such helical fibers is accountable for the gelation of amphiphile **3a** in ethanol. Additional support for this assumption came from the fact that the SEM images of the solid revealed the presence of fibers with an identical helical twist. Of course, further detailed studies covering various aspects of these gels are under way. These results suggest that the molecules in their solid, LC, and gel states self-assemble in macroscopic chiral (helical) structures.

or discotics) are currently in the limelight, and importantly, their usage as a possible media for different applications has been demonstrated.[26b] Particularly, LC physical gels composed of supramolecules, namely, amino acid derivatives (as gelators) are of special significance for various technological reasons.[26b,27] In this context, it would be interesting to know whether amino acid derivatives **3a–c** and **4a–c**, which are amphiphilic systems, form stable organogels. Thus, the preliminary investigation on the gelation ability of all the synthesized LC homomeric dipep-

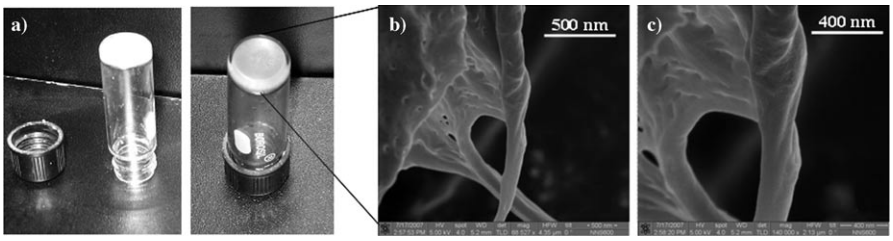

Figure 9. a) The demonstration of the formation of a stable organogel by dipeptide **3b** in ethanol. Note that the sample does not flow when its container is inverted. b, c) SEM images obtained for the gel.

Conclusion

We have demonstrated that several homomeric dipeptides derived from proteinogenic α-amino acids can be made to exhibit electrically switchable novel fluid supramolecular aggregates, in which the ordering in the columns facilitated by hydrogen bonding, are essentially controlled by the stereochemistry encoded (chirality) in the peptide chain. Interestingly, the enantiomers and their diastereomers behave differently, in particular, the clearing-point temperature values of diastereomers are nearly half of those noted for the corresponding enantiomers, which can be attributed to the orientation of the alkyl groups (methyl and isobutyl) present in the amino acid (alanine and leucine) residues. The creation of such low molar mass, monodisperse, mesogen oligopeptides with gelating ability may lead to the induction of dynamically functional properties on the molecular and macroscopic levels. These may also be regarded as biocompatible fluids for use in membranes and sensors. If these LCs form composites with a lipid membrane, they could facilitate the transport of ions and amino acids. Thus the homomeric dipeptides described herein are early examples of what could be a vast family of materials that may find applications in high-tech and biorelated fields.

Acknowledgements

We sincerely thank Prof. G. U. Kulkarni (JNCASR, Bangalore) for providing SEM images for our samples and Prof. Uday Maitra (IISc, Bangalore) for very helpful discussions. We are also grateful to S. D. Hombal (CLCR, Bangalore) and N. R. Selvi (JNCASR, Bangalore) for their technical assistance.

[1] a) J.-M. Lehn, *Supramolecular Chemistry*, Wiley-VCH, Weinheim, **1995**; b) O. Ikkala, G. ten Brinke, *Science* **2002**, *295*, 2407–2409.

[2] S. Chandrasekhar, B. K. Sadashiva, K. A. Suresh, *Pramana* **1977**, *9*, 471–480.

[3] a) R. J. Bushby, O. R. Lozman, *Curr. Opin. Colloid Interface Sci.* **2002**, *7*, 343–354; b) S. Laschat, A. Baro, N. Steinke, F. Giesselmann, C. Hagele, G. Scalia, R. Judele, E. Kapatsina, S. Sauer, A. Schreivogel, M. Tosoni, *Angew. Chem.* **2007**, *119*, 4916–4973; *Angew. Chem. Int. Ed.* **2007**, *46*, 4832–4887.

[4] a) G. Pelzl, S. Diele, W. Weissflog, *Adv. Mater.* **1999**, *11*, 707–724; b) R. Amaranatha Reddy, C. Tschierske, *J. Mater. Chem.* **2006**, *16*, 907–961.

[5] M. Gharbia, A. Gharbi, H.-T. Nguyen, J. Malthete, *Curr. Opin. Colloid Interface Sci.* **2002**, *7*, 312–325.

[6] a) V. Percec, M. Glodde, T. K. Bera, Y. Miura, I. Shiyanovskaya, K. D. Singer, V. S. K. Balagurusamy, P. A. Heiney, L. Schnell, A. Rapp, H.-W. Spiess, S. D. Hudson, H. Daun, *Nature* **2002**, *417*, 384–387; b) H. Meier, M. Lehmann, *Angew. Chem.* **1998**, *110*, 666–669; *Angew. Chem. Int. Ed.* **1998**, *37*, 643–645; c) M. Marcos, R. Gimennez, J. L. Serrano, D. Bertrand, B. Heinrich, D. Guillon, *Chem. Eur. J.* **2001**, *7*, 1006–1013.

[7] B. Chen, X. Zeng, U. Baumeister, G. Ungar, C. Tschierske, *Science* **2005**, *307*, 96–98.

[8] a) M. Prehm, S. Diele, M. K. Das, C. Tschierske, *J. Am. Chem. Soc.* **2003**, *125*, 614–615; b) X. Cheng, M. Prehm, M. K. Das, J. Kain, U. Baumeister, S. Diele, D. Leine, A. Blume, C. Tschierske, *J. Am. Chem. Soc.* **2003**, *125*, 10996–10996.

[9] a) T. Kato, *Science* **2002**, *295*, 2414–2418; b) For a recent review on columnar liquid crystals with hydrogen bonds, see: L. Brunsfeld, B. J. B. Folmer, E. W. Meijer, R. P. Sijbesma, *Chem. Rev.* **2001**, *101*, 4071–4097; c) L. J. Prins, D. N. Reinhoudt, P. Timmerman, *Angew. Chem. Int. Ed.* **2001**, *40*, 2383–2426.

[10] a) T.-Q. Nguyen, M. L. Bushey, L. E. Brus, C. Nuckolls, *J. Am. Chem. Soc.* **2002**, *124*, 15051–15054; b) J. J. van Grop, J. A. J. M. Vekemans, E. W. Meijer, *J. Am. Chem. Soc.* **2002**, *124*, 14759–14769; c) R. I. Gearba, M. Lehmann, J. Levin, D. A. Ivanov, M. H. J. Koch, J. Barbera, M. G. Debije, J. Piris, Y. H. Greets, *Adv. Mater.* **2003**, *15*, 1614–1618; d) K. Kishikawa, S. Nakahara, Y. Nishikawa, S. Kohmoto, M. Yamamoto, *J. Am. Chem. Soc.* **2005**, *127*, 2565–2571, and references therein; e) V. Percec, C.-H. Ahn, T. K. Bera, G. Ungar, D. J. P. Yeardley, *Chem. Eur. J.* **1999**, *5*, 1070–1083.

[11] a) J. van Gestel, A. R. A. Palmans, B. Titulaer, J. A. J. M. Vekemans, E. W. Meijer, *J. Am. Chem. Soc.* **2005**, *127*, 5490–5494; b) C. Xue, X. Weng, J.-J. Ge, Z. Shen, H. Shen, M. J. Graham, K.-U. Jeong, H. Huang, D. Zhang, M. Guo, F. W. Harris, S. Z. D. Cheng, *Chem. Mater.* **2004**, *16*, 1014–1025; c) M. L. Bushey, A. Hwang, P. W. Stephend, C. Nuckolls, *Angew. Chem.* **2002**, *114*, 2952–2955; *Angew. Chem. Int. Ed.* **2002**, *41*, 2828–2831; d) A. R. A. Palmans, J. A. J. M. Vekemans, E. E. Havinga, E. W. Meijer, *Angew. Chem.* **1997**, *109*, 2763–2765; *Angew. Chem. Int. Ed. Engl.* **1997**, *36*, 2648–2651; e) U. Kumar, T. Kato, J. M. J. Frechet, *J. Am. Chem. Soc.* **1992**, *114*, 6630–6639; f) S. Qu, F. Li, H. Wang, B. Bai, C. Xu, L. Zhao, B. Long, M. Li, *Chem. Mater.* **2007**, *19*, 4839–4846.

[12] W. Zhou, W. Gu, Y. Xu, C. S. Pecinovsky, D. L. Gin, *Langmuir* **2003**, *19*, 6346–6348.

[13] a) V. Percec, M. R. Imam, T. K. Bera, V. S. K. Balaguruswamy, M. Peterca, P. A. Heiney, *Angew. Chem.* **2005**, *117*, 4817–4823; *Angew. Chem. Int. Ed.* **2005**, *44*, 4739–4745; b) V. Percec, T. K. Bera, M. Glodde, Q. Fu, V. S. K. Balagurusamy, P. A. Heiney, *Chem. Eur. J.* **2003**, *9*, 921–935.

[14] J. Watanabe, Y. Takashina, *Macromolecules* **1991**, *24*, 3423–3426, and references therein.

[15] a) V. Percec, A. E. Dulcey, V. S. K. Balaguruswamy, Y. Miura, J. Smidrkal, M. Peterca, S. Nummelin, U. Edlund, S. D. Hudson, P. A. Heiney, H. Duan, S. N. Magonov, S. Vinogradov, *Nature* **2004**, *430*, 764–768; b) V. Percec, A. E. Dulcey, M. Peterca, M. Ilies, J. Ladislaw, B. M. Rosen, U. Edlund, P. A. Heiney, *Angew. Chem.* **2005**, *117*, 6674–6679; *Angew. Chem. Int. Ed.* **2005**, *44*, 6516–6521; c) M. Peterca, V. Percec, A. E. Dulcey, S. Nummelin, S. Korey, M. Llies, P. A. Heiney, *J. Am. Chem. Soc.* **2006**, *128*, 6713–6720.

[16] a) M. Nishii, T. Matsuoka, Y. Kamikawa, T. Kato, *Org. Biomol. Chem.* **2005**, *3*, 875–880; b) T. Kato, T. Matsuoka, M. Nishi, Kamikawa, K. Kanie, T. Nisjimura, E. Yashima, S. Ujiie, *Angew. Chem.* **2004**, *116*, 2003–2006; *Angew. Chem. Int. Ed.* **2004**, *43*, 1969–1972; c) T. Kato, N. Mizoshita, K. Kishimoto, *Angew. Chem.* **2006**, *118*, 44–74; *Angew. Chem. Int. Ed.* **2006**, *45*, 38–68.

[17] a) J. Venkatraman, S. C. Shankaramma, P. Balaram, *Chem. Rev.* **2001**, *101*, 3131–3152; b) De. M. Chung, Y. Dou, P. Baldi, J. S. Nowick, A. C. Griffin, T. R. Britt, *J. Am. Chem. Soc.* **2005**, *127*, 9998–9999; c) H. Shen, K.-U. Jeong, M. J. Graham, S. Leng, J. X. Zheng, H. Huang, M. Guo, F. W. Harris, S. Z. D. Cheng, *Soft Matter* **2006**, *2*, 232–242; d) M. Suzuki, T. Sato, H. Shirai, K. Hanabusa, *New J. Chem.* **2006**, *30*, 1184–1191.

[18] a) F. Morale, R. W. Date, D. Guillon, D. W. Bruce, R. L. Finn, C. Wilson, A. J. Blake, M. Schröder, B. Donnio, *Chem. Eur. J.* **2003**, *9*, 2484–2501.

[19] a) A. V. Petukhov, D. van der Beek, R. P. A. Dullens, I. P. Dolbnya, G. V. Vroege, H. N. W. Lekkerkerker, *Phys. Rev. Lett.* **2005**, *95*, 77801–77804; b) J. Barbera, R. Iglesias, J. L. Serrano, T. Sierra, M. R. de la Fuente, B. Palacios, M. A. Perez-Jubindo, J. T. Vazquez, *J. Am. Chem. Soc.* **1998**, *120*, 2908–2918.

[20] M. Lehmann, G. Kestemont, R. Gómez Aspe, C. Buess-Hermann, M. H. J. Koch, M. G. Debije, J. Piris, M. P. de Haas, J. M. Warman, M. D. Watson, V. Lemaur, J. Cornil, Y. H. Geerts, R. Gearba, D. A. Ivanov, *Chem. Eur. J.* **2005**, *11*, 3349–3362.

[21] B. Donnio, B. Heinrich, H. Allouchi, J. Kain, S. Diele, D. Guillon, D. W. Bruce, *J. Am. Chem. Soc.* **2004**, *126*, 15258–15268.
[22] a) H. Bock, W. Helfrich, *Liq. Cryst.* **1992**, *12*, 697–703; b) H. Bock, W. Helfrich, *Liq. Cryst.* **1995**, *18*, 387–399; c) H. Bock, W. Helfrich, *Liq. Cryst.* **1995**, *18*, 707–713; d) H. Takezoe, K. Kishikawa, E. Gorecka, *J. Mater. Chem.* **2006**, *16*, 2412–2416; e) H. Kitzerow, C. Bahr, *Chirality in Liquid Crystals*, Springer, New York, **2001**; f) *Topics in Stereochemistry: Materials-Chirality, Vol. 24* (Eds.: M. M. Green, R. J. M. Nolte, E. W. Meijer), Wiley, Hoboken, **2003**, Chapter 6.
[23] a) J. Malthete, A. Collet, *J. Am. Chem. Soc.* **1987**, *109*, 7544–7545; b) A. Jakli, A. Saupe, *Liq. Cryst.* **1997**, *22*, 309–316.
[24] A. G. Serrette, T. M. Swager, *Angew. Chem.* **1994**, *106*, 2378–2380; *Angew. Chem. Int. Ed. Engl.* **1994**, *33*, 2342–2435.
[25] M. Sawamura, K. Kawai, Y. Matsuo, K. Kanie, T. Kato, E. Nakamura, *Nature* **2002**, *419*, 702–705.
[26] a) P. Terech, R. G. Weiss, *Chem. Rev.* **1997**, *97*, 3133–3159; b) N. M. Sangeetha, U. Maitra, *Chem. Soc. Rev.* **2005**, *34*, 821–836.
[27] a) N. Mizoshita, H. Monobe, M. Inoue, M. Ukon, T. Watanabe, Y. Shimizu, K. Hanabusa, T. Kato, *Chem. Commun.* **2002**, 428–429; b) N. Mizoshita, Y. Suzuki, K. Kishimoto, K. Hanabusa, T. Kato, *J. Mater. Chem.* **2002**, *12*, 2197–2201; c) F. Camerel, G. Ulrich, R. Ziessel, *Org. Lett.* **2004**, *6*, 4171–4174.
[28] S. G. Lim, B. M. Jung, L. S. Lee, H. H. Song, C. Kim, Y. J. Chang, *Chem. Mater.* **2007**, *19*, 460–467, and references therein.
[29] a) S. Kobayashi, N. Hamasaki, M. Suzuki, M. Kimura, H. Shirai, K. Hanabusa, *J. Am. Chem. Soc.* **2002**, *124*, 6550–6551; b) Y. Yang, M. Nakazawa, M. Suzuki, H. Shirai, K. Hanabusa, *J. Mater. Chem.* **2007**, *17*, 2936–2943; c) Y. Ono, K. Nakashima, M. Sano, Y. Kanekiyo, K. Inoue, H. Junichi, S. Shinkai, *Chem. Commun.* **1998**, 1477–1478.

Received: August 4, 2008
Published online: October 1, 2008

